Magnetocaloric effect in spin-degenerated molecular nanomagnets

Magnetocaloric effect in spin-degenerated molecular nanomagnets

M. Evangelisti,[1,*] A. Candini,[1] M. Affronte,[1,2] E. Pasca,[3] L. J. de Jongh,[3] R. T. W. Scott,[4] and E. K. Brechin[4]
[1]*National Research Center on "nanoStructures and bioSystems at Surfaces" (S3), CNR-INFM, 41100 Modena, Italy*
[2]*Dipartimento di Fisica, Università di Modena e Reggio Emilia, 41100 Modena, Italy*
[3]*Kamerlingh Onnes Laboratory, Leiden University, 2300 RA Leiden, The Netherlands*
[4]*School of Chemistry, The University of Edinburgh, EH9 3JJ Edinburgh, United Kingdom*
(Received 17 November 2008; revised manuscript received 2 February 2009; published 12 March 2009)

For molecular nanomagnets, excesses of magnetic entropy at finite low temperatures are induced by degrees of freedom resulting from macroscopic degeneracies of the molecular spin states. We experimentally demonstrate that this effect can be huge and efficiently exploited for enhancing the magnetic field dependence of the adiabatic temperature change. We specifically consider the Mn_{32} molecular nanomagnet, proving it to be an excellent magnetic refrigerant below $T \approx 2$ K, due almost entirely to its spin degeneracy.

DOI: 10.1103/PhysRevB.79.104414 PACS number(s): 75.50.Xx, 75.10.−b, 75.30.Sg, 75.40.Cx

I. INTRODUCTION

Molecular nanomagnets can potentially show a very large magnetocaloric effect (MCE) at low temperatures[1–4] and are thus attractive materials for magnetic refrigeration technology.[5] Relevant applications are, for instance, in ultralow-temperature radiation detectors for outer space research, where the absence of gravity makes difficult the use of conventional ^{3}He-^{4}He dilution refrigerators. High-spin molecules with vanishing magnetic anisotropy are particularly favorable since: (i) the higher the spin value the larger the density of spin levels and thus the larger the magnetic entropy content; (ii) a negligible anisotropy permits easy polarization of the net molecular spins in magnetic fields of weak or moderate strength.[2,6] Another property favoring large MCE is the presence of degenerate or low-lying spin states induced, e.g., by frustration, as was recently pointed out by Schnack *et al.*[7] and Zhitomirsky,[8] who concluded that in terms of MCE the field-dependent efficiency of a geometrically frustrated magnet can exceed that of an ideal paramagnet with equivalent spin by more than an order of magnitude. In this regard recent results obtained for the magnetically frustrated Fe_{14} molecular cluster compound are indeed quite promising.[9,10]

An alternative and perhaps simpler approach to frustration in promoting spin degeneracy is by designing very weak magnetic links between the single-ion spin centers. Herein, we study the MCE of the molecular magnetic cluster compound Mn_{32} that perfectly meets the above requirements of a large number of low-lying spin states and a small magnetic anisotropy, making this material an ideal refrigerant for very-low-temperature applications. The magnetically relevant structure[11] of the Mn_{32} molecule consists of eight planar "centered triangles" composed of a central Mn^{4+} ion, with spin $s=3/2$, antiferromagnetically coupled to three peripheral Mn^{2+} ions, each having spin of $s=5/2$ (Fig. 1). Within the molecule the eight triangular clusters, each with net spin of $S=6$, are weakly coupled together in the form of a truncated cube by azide and carboxylate ligands, which are known to promote very weak magnetic interaction.[11] Each Mn_{32} core is also surrounded by one-and-a-half noncoordinated $[Mn(bpy)_3]^{2+}$. The full formula of the molecular complex reads

$$\{Mn(bpy)_3\}_{1.5}[Mn_{32}(thme)_{16}(bpy)_{24}(N_3)_{12}(OAc)_{12}](ClO_4)_{11}.$$

Magnetic interactions between neighboring Mn_{32} molecules in the crystal are much weaker still. At $T \approx 1$ K the magnetization per Mn_{32} molecule reaches the huge value of $50\mu_B$ already in a moderate field of $B_0=1$ T. The anisotropy is so small that superparamagnetic blocking does not occur; instead a transition to a three-dimensional (3D) long-range magnetic order between the Mn triangles is found below 0.32 K from specific-heat measurements.

Magnetization measurements down to 2 K and specific-heat measurements using the relaxation method down to ≈ 0.35 K on powder samples were carried out in Modena by means of a commercial setup for the $0 < B_0 < 7$ T magnetic field range. Magnetization measurements below 2 K were performed using a homemade Hall microprobe installed in the same setup. In this case the sample consisted of a collection of small grains of c.a. 10^{-3} mm^3. Specific-heat experiments on powder samples were extended down to 0.1 K with a homemade calorimeter using the relaxation method, installed in a dilution refrigerator at Leiden University.

II. EXPERIMENTAL RESULTS AND DISCUSSION

Preliminary magnetic characterizations[11] of the Mn_{32} molecule already suggested the presence of many low-lying excited spin states. Here we report highly detailed magnetiza-

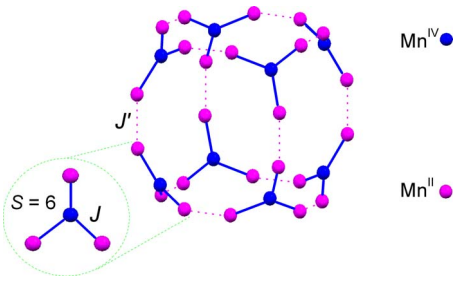

FIG. 1. (Color online) The metallic skeleton of the Mn_{32} molecule, emphasizing the centered triangle $[Mn^{IV}Mn^{II}_3]$ building block. The exchange couplings depicted as solid and dotted lines are J and J', respectively.

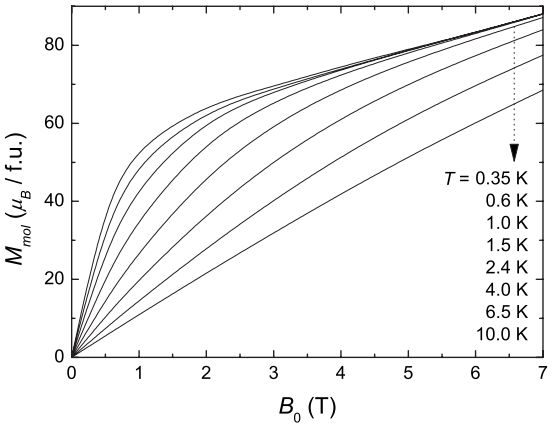

FIG. 2. Field dependencies of the experimental molar magnetization for several temperatures as listed.

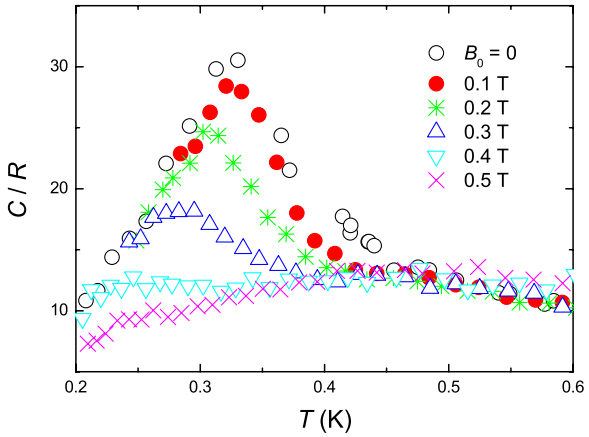

FIG. 3. (Color online) Temperature dependencies of the low-T specific heat C normalized to the gas constant R collected for applied magnetic field B_0=0, 0.1, 0.2, 0.3, 0.4, and 0.5 T, as labeled. The peak in the zero-field data observed at T_c=0.32 K indicates a phase transition to long-range magnetic order. This feature gradually shifts with increasing field and is finally suppressed for $B_0 \simeq 0.5$ T.

tion measurements that corroborate and extend the previous results. Figure 2 shows the measured molar magnetization in fields up to 7 T for temperatures down to ≈0.35 K, at which temperature a value as high as 87 $N\mu_B$ is reached. Assuming g=2 for both the Mn^{2+} and Mn^{4+} ions, this value is indeed compatible with a field-induced $S \gtrsim 43$ spin state, not far from the S_{tot}=48 spin state expected for a parallel alignment of the eight S=6 spin triangles in the molecule. Judging from the shape of the magnetization curves at lowest temperature (see also inset in Fig. 3 of Ref. 11), the magnetic coupling between the triangles inside the molecule (J') as well as the much weaker intermolecular interaction between molecules are both antiferromagnetic. The sharp initial rise seen below 1 T probably arises from a sizable canted moment (incompletely compensated antiferromagnetism). Evidently, the magnetization reached in 7 T is still far from the saturation value of 144 $N\mu_B$ calculated for 24 Mn^{2+} and 8 Mn^{4+} paramagnetic ions per molecule, i.e., appropriate for noninteracting spins. The finite slope of the magnetization curve remaining in high field can therefore be attributed as arising from the gradual decoupling of the antiferromagnetic interaction within the triangles (J is the strongest exchange interaction present in the structure).

Figure 3 shows the measured low-temperature specific-heat C/R data as a function of temperature for several applied fields. The main feature is the peak in the zero-field data observed at T_c=0.32 K, indicating a phase transition to long-range magnetic order. Its magnetic origin is indeed proved by the fact that this feature is quickly and fully suppressed in external fields $B_0 \gtrsim 0.5$ T. The effect of further increasing B_0 is to shift the magnetic contribution to the specific heat toward higher temperatures (Fig. 4). In agreement with the $M(T,B_0)$ data, the analysis of the field-dependent heat capacity reveals that magnetic interactions between single-ion spin centers are relatively weak, though applied fields of up to 7 T are not yet sufficient to fully decouple all of them. As a comparison with the experimental data, Fig. 4 (top) shows the contributions (solid lines for B_0=1, 3 and 7 T, respectively) that result by summing together the Schottky curves arising from the field-split levels of 25.5 Mn^{2+} and 8 Mn^{4+} independent spins. It can be seen that the calculated B_0=1 T curve fails completely to describe the experimental behavior. However, higher fields promote a larger decoupling between the individual spin centers, yielding thus to an increasingly much better agreement, as indeed shown in the Fig. 4. In the high-temperature range above 6 K a large field-independent contribution appears, which can be attributed to

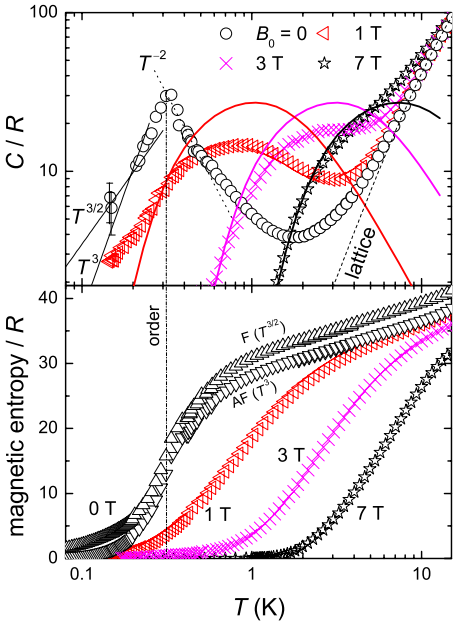

FIG. 4. (Color online) Top: temperature dependencies of the specific heat C normalized to the gas constant R collected for B_0 =0, 1, 3, and 7 T, as labeled. Solid thick lines are the sums of the calculated Schottky contributions of all independent spins; dashed line is the fitted lattice contribution; and dotted line is the high-T dependence ($\propto T^{-2}$) of the zero-field magnetic anomaly. Plotted also are the extrapolated spin-wave contributions ($\propto T^3$ and $T^{3/2}$), as labeled. Bottom: T dependencies of the experimental magnetic entropies for several B_0, as obtained from the respective magnetic contributions C_m to the total specific heat.

the lattice phonon modes of the crystal. The dashed line in Fig. 4 (top) represents a fit to this contribution, with the well-known low-T Debye function yielding a value of $\Theta_D = 15$ K for the Debye temperature, as is typical for this class of weakly coupled cluster compounds.[3]

The occurrence of long-range magnetic order implies a negligible molecular magnetic anisotropy; otherwise superparamagnetic blocking would have occurred at a more elevated temperature, thereby inhibiting the phase transition.[12] Indeed, dc-susceptibility measurements carried out down to 0.35 K showed no sign of superparamagnetic blocking. The argument is particularly strong in view of the very low value of T_c. In terms of MCE, we remind that negligible anisotropy is particularly favorable for obtaining large magnetic entropy changes.[2,6] In addition, since maximum entropy changes are found at magnetic ordering temperatures, phase transitions are also favorable for enhanced MCE.[5,13] From the experimental specific heat (Fig. 4) the temperature dependence of the magnetic entropy $S_m(T)$ is obtained by integration, i.e., using

$$S_m(T) = \int_0^T \frac{C_m(T)}{T} dT, \tag{1}$$

where $C_m(T)$ is the magnetic specific heat as obtained by subtracting the lattice contribution to the total C measured. The so-obtained $S_m(T)$ is shown in the bottom panel of Fig. 4 for the corresponding applied fields. The results obtained slightly depend on the extrapolation to $T=0$ chosen for the data, especially for $B_0=0$ because of their larger values. As indicated in the Fig. 4 we have used for the zero-field data either a $\propto T^3$ or $\propto T^{3/2}$ dependence, as would be appropriate for the spin-wave contributions for an isotropic 3D antiferromagnet or ferromagnet, respectively. We note that the zero-field entropy value attained at and just above T_c is of considerable importance within the present context since it gives a direct determination of the value of the spin state involved in the magnetic phase transition through the following relation:

$$\Delta S_m = R \ln(2S+1). \tag{2}$$

Assuming the antiferromagnetic interactions between the central Mn^{4+} ion and the three peripheral Mn^{2+} ions in each triangle to be strong enough to yield a well-defined $S=6$ state below 1 K, ordering of these $S=6$ spins *within and between* the Mn_{32} molecules would yield an entropy change $8 \times R \ln 13 = 20.5R$, in good agreement with the experimental value found near 0.4 K. As the temperature is further increased above this value the entropy content associated with the antiferromagnetic ordering within the triangles is gradually removed, as seen by the continuously increasing experimental $S_m(T)$ curves. The maximum entropy value per mole involved, corresponding to 8 Mn^{4+} spins $s=3/2$ and 25.5 Mn^{2+} spins $s=5/2$ is calculated as $56.7R$. This value is not reached experimentally since the determination of the magnetic $S_m(T)$ becomes too uncertain above $T \approx 8$ K. In addition, we point out that assigning the phase transition to be due to a purely *intermolecular* magnetic ordering process, i.e., assuming full magnetic order between the eight spin $S=6$ triangles inside each molecule, would lead to a maximum $\Delta S_m = R[\ln(2S_{\text{tot}}+1) + 1.5 \times \ln 6] \simeq 7.3R$ only, even when adopting the highest possible total spin $S_{\text{tot}}=48$/molecule obtained in case of ferromagnetic alignment.

Having thus established a model for the magnetic structure of the Mn_{32} molecule, we next evaluate the magnetic interaction constants. For the antiferromagnetic coupling J inside the triangles (Fig. 1), we can use the value of the slope of the magnetization curve at highest fields and lowest temperature, $\chi_{\text{HF}} = \partial M / \partial H \approx 4.5 \times 10^{-4} N \mu_B G^{-1}$, as argued above. Equating this to the theoretical perpendicular susceptibility of the Heisenberg antiferromagnet,

$$\chi_\perp = \frac{N g^2 \mu_B^2}{4z|J|}, \tag{3}$$

with $z=3$ the number of exchange-coupled Mn^{2+}-Mn^{4+} pairs inside each triangle, gives $J/k_B \approx 0.07$ K. With regard to the coupling *between* the spins $S=6$ of the triangles, it is not possible to distinguish between intramolecular (J' in Fig. 1) and intermolecular interactions; only an average $\hat{J}$ can be found. A first estimate is obtained by comparing the experimental T^{-2} term, $CT^2/R = 2.9$ K^2 to the theoretical expression for the high-temperature tail of the magnetic specific heat, i.e.,

$$\frac{CT^2}{R} = 2n\hat{z}\left[\frac{S(S+1)|\hat{J}|}{3k_B}\right]^2, \tag{4}$$

where $\hat{z}$ is the number of nearest magnetic neighbors between different triangles and $n=1$, 2, and 3 for Ising, XY, and Heisenberg models, respectively.[14] This comparison provides $\hat{z}^{1/2}\hat{J}/k_B = 0.05$ K. Using the mean-field expression for the transition temperature,

$$T_c = \frac{2\hat{z}|\hat{J}|S(S+1)}{3k_B}, \tag{5}$$

one finds from $T_c = 0.32$ K a value $\hat{z}\hat{J}/k_B = 0.01$ K. This is probably an underestimate since usually the actual transition temperature is appreciably lower than the mean-field prediction. From the experimental value of the critical field needed to fully suppress the magnetic ordering anomaly, $B_c \simeq 0.5$ T, and using the prediction

$$B_c = \frac{2\hat{z}|\hat{J}|S}{g\mu_B} \tag{6}$$

for the Heisenberg antiferromagnet, we obtain $\hat{z}\hat{J}/k_B = 0.03$ K. One may conclude that the interactions inside the triangles are indeed substantially larger than those between them but that the difference is not that large, in agreement with the above discussed temperature dependence of the entropy.

III. EVALUATION OF THE MAGNETOCALORIC EFFECT

We next evaluate the MCE for the Mn_{32} molecular complex. This procedure includes the calculation of the isothermal magnetic entropy change ΔS_m and adiabatic temperature

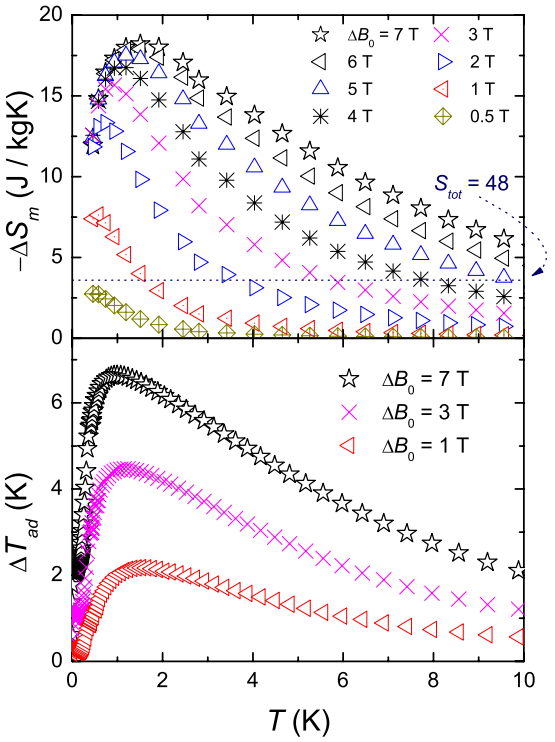

FIG. 5. (Color online) Top: T dependencies of the magnetic entropy change $\Delta S_m(T)$ as obtained from magnetization data (Fig. 2) for the indicated applied-field changes ΔB_0. Dotted line is the limiting entropy assuming paramagnetic $S_{\text{tot}}=48$. Bottom: T dependencies of the adiabatic temperature change ΔT_{ad} as obtained from heat-capacity data (Fig. 3) for the indicated ΔB_0.

change ΔT_{ad}, following a change in the applied magnetic field ΔB_0, from the measured magnetization and specific heat, respectively. In an isothermal process of magnetization, ΔS_m can be derived from Maxwell relations by integrating over $\Delta B_0 = B_f - B_i$; that is,

$$\Delta S_m(T)_{\Delta B_0} = \int_{B_i}^{B_f} \left[\frac{\partial M(T,B_0)}{\partial T} \right]_{B_0} dB_0. \tag{7}$$

From the $M(T,B_0)$ data of Fig. 2, the obtained $\Delta S_m(T)$ for several ΔB_0 is displayed in Fig. 5 (top).[15] It can be seen that $-\Delta S_m(T)$ reaches a remarkable maximum of 18.2 J kg^{-1} K^{-1} (equivalent to $23.2R$) at $T \simeq 1.6$ K for $\Delta B_0 = (7-0)$ T and that this maximum decreases both in magnitude as well in temperature by decreasing ΔB_0. The adiabatic temperature change can be estimated as

$$\Delta T_{\text{ad}}(T)_{\Delta B_0} = [T(S_m)_{B_f} - T(S_m)_{B_i}]_{S_m} \tag{8}$$

directly from the experimental magnetic entropy S_m depicted in Fig. 4, which we previously obtained from the heat-capacity data. Note that the uncertainty in the determination of the field-independent lattice contribution is irrelevant for these calculations and cancels out since we deal with differences between entropies. Figure 5 (bottom) shows that $\Delta B_0 = (7-0)$ T provides a maximum $\Delta T_{\text{ad}} = 6.7$ K for the same temperature range in which we observe the $-\Delta S_m$ maxima. By lowering ΔB_0 to $(3-0)$ and $(1-0)$ T, ΔT_{ad} decreases down to 4.5 and 2.2 K, respectively. In contrast the magnetic field dependence of the adiabatic temperature change increases from ≈ 1 to over 2 K/T, respectively, setting this material among the most efficient refrigerants for this low-temperature range.[5]

Let us compare these results with the hypothetical situation in which for the whole investigated temperature and field range Mn_{32} would possess a large well-defined molecular spin ground state, e.g., the highest possible total spin $S_{\text{tot}}=48$. In that case, ΔS_m could not exceed the full magnetic entropy content of $R \ln(2S_{\text{tot}}+1)$, which corresponds to 3.6 J kg^{-1} K^{-1} only and is depicted in Fig. 5 (top) together with the experimental results for comparison. Clearly, the experimental ΔS_m ridicules this hypothetical limit since it is seen to become about *five times* larger for $\Delta B_0 = (7-0)$ T. We can conclude that the macroscopic degeneracy of the molecular spin states is playing the dominating role in determining the MCE of the Mn_{32} molecular complex, being a much more important factor than the (field-stabilized) high-spin value[1,9] or the negligible anisotropy.[2,6]

IV. CONCLUSIONS

In conclusion, we have shown that with Mn_{32} the emerging field of low-temperature magnetic refrigeration using molecule-based materials has clearly been enriched with an excellent candidate. In particular, Mn_{32} is the best performing material found so far, when cooled down to (1–2) K as the starting range for the adiabatic demagnetization. The latter range is of considerable technological interest because it is easily reachable by pumping liquid ^{4}He. From the pure scientific point of view Mn_{32} provides a rare example of an enhanced MCE almost entirely due to macroscopic spin degeneracy. As we have shown this arises from its relatively high nuclearity, in combination with the weak magnetic interactions between and within the triangular spin units that compose the magnetic core of the molecular clusters.

ACKNOWLEDGMENTS

The authors are indebted to F. Troiani for helpful discussions. This work is partially funded by the EC-Network of Excellence "MAGMANet" (Contract No. 515767).

*Author to whom correspondence should be addressed. Present address: ICMA, CSIC-Universidad de Zaragoza, 50009 Zaragoza, Spain.

[1] Yu. I. Spichkin, A. K. Zvezdin, S. P. Gubin, A. S. Mischenko, and A. M. Tishin, J. Phys. D **34**, 1162 (2001), and references therein.

[2] For an overview, see, e.g., M. Evangelisti, F. Luis, L. J. de Jongh, and M. Affronte, J. Mater. Chem. **16**, 2534 (2006) and references therein.

[3] M. Manoli, R. D. L. Johnstone, S. Parsons, M. Murrie, M. Affronte, M. Evangelisti, and E. K. Brechin, Angew. Chem., Int. Ed. **46**, 4456 (2007).

[4] M. Manoli, A. Collins, S. Parsons, A. Candini, M. Evangelisti, and E. K. Brechin, J. Am. Chem. Soc. **130**, 11129 (2008).

[5] For an overview, see, e.g., V. K. Pecharsky and K. A. Gschneidner, Jr., J. Magn. Magn. Mater. **200**, 44 (1999), and references therein.

[6] X. X. Zhang, H. L. Wei, Z. Q. Zhang, and L. Zhang, Phys. Rev. Lett. **87**, 157203 (2001).

[7] J. Schnack, R. Schmidt, and J. Richter, Phys. Rev. B **76**, 054413 (2007).

[8] M. E. Zhitomirsky, Phys. Rev. B **67**, 104421 (2003).

[9] M. Evangelisti, A. Candini, A. Ghirri, M. Affronte, E. K. Brechin, and E. J. L. McInnes, Appl. Phys. Lett. **87**, 072504 (2005).

[10] R. Shaw, R. H. Laye, L. F. Jones, D. M. Low, C. Talbot-Eeckelaers, Q. Wei, C. J. Milios, S. Teat, M. Helliwell, J. Raftery, M. Evangelisti, M. Affronte, D. Collison, E. K. Brechin, and E. J. L. McInnes, Inorg. Chem. **46**, 4968 (2007).

[11] R. T. W. Scott, S. Parsons, M. Murugesu, W. Wernsdorfer, G. Christou, and E. K. Brechin, Angew. Chem., Int. Ed. **44**, 6540 (2005).

[12] M. Evangelisti, A. Candini, A. Ghirri, M. Affronte, G. W. Powell, I. A. Gass, P. A. Wood, S. Parsons, E. K. Brechin, D. Collison, and S. L. Heath, Phys. Rev. Lett. **97**, 167202 (2006).

[13] E. Manuel, M. Evangelisti, M. Affronte, M. Okubo, C. Train, and M. Verdaguer, Phys. Rev. B **73**, 172406 (2006); M. Evangelisti, E. Manuel, M. Affronte, M. Okubo, C. Train, and M. Verdaguer, J. Magn. Magn. Mater. **316**, e569 (2007).

[14] A. Abragam and B. Bleaney, *Electron Paramagnetic Resonance of Transition Ions* (Oxford University Press, Oxford, England, 1970).

[15] For practical reasons, the measurements at the lowest applied field were carried out for B_i=0.01 T, which in our calculations was approximated to zero-applied field.